A random-key genetic algorithm-based method for transportation network vulnerability envelope analysis under simultaneous multi-link disruptions

Yu Gu[1], Seungkyu Ryu[2], Yingying Xu[1], Anthony Chen[1,3*], Ho-Yin Chan[4], Xiangdong Xu[5]

[1] Department of Civil and Environmental Engineering, The Hong Kong Polytechnic University, Hong Kong.
[2] Korea Institute of Science and Technology Information, Daejeon, South Korea.
[3] The Hong Kong Polytechnic University Shenzhen Research Institute, Shenzhen, Guangdong, China.
[4] Transport Studies Unit, School of Geography and the Environment University of Oxford, UK
[5] College of Transportation Engineering, Tongji University, Shanghai, China

Email:
Yu Gu: frank.gu@connect.polyu.hk;
Seungkyu Ryu: ryuseungkyu@kisti.re.kr;
Yingying Xu: ying.y.xu@connect.polyu.hk;
Anthony Chen:
anthony.chen@polyu.edu.hk; Ho-Yin Chan:
ho.chan@ouce.ox.ac.uk; Xiangdong Xu:
xiangdongxu@tongji.edu.cn;

* Corresponding author: anthony.chen@polyu.edu.hk

Highlights

- Bi-level program model for determining upper and lower bounds of transportation network vulnerability envelope
- A random-key genetic algorithm-based method for solving the bi-level model
- Identification of both most important and sub-important link combinations
- Simultaneous measurement of lower and upper vulnerability bounds together with their buffers
- Application to vulnerability analyses of real-world networks with different sizes

Abstract

Transportation network vulnerability envelope (TNVE), constituted by the upper and lower bounds of network performance among all possible disruption scenarios, has recently been proposed as a systematic tool to characterize the impact of simultaneous disruptions of multiple links in a transportation network. Both pessimistic and optimistic cases and the possible range of disruption consequences can be revealed by the TNVE, which can be modeled as a unified optimization problem without the need to enumerate and evaluate all possible disruption scenarios. Specifically, the TNVE problem can be formulated as a binary integer bi-level program (BLP), in which the upper-level problem maximizes/minimizes the remaining network performance under a given number of disrupted links, and the lower-level problem adopts the shortest path problem to check the post-disruption connectivity of each origin- destination (O-D) pair while circumventing the cumbersome path enumeration or path set pre- generation. However, the binary integer BLP is computationally intractable, which hinders the applications of TNVE in practice. This study aims to develop an efficient method based on the random key genetic algorithm (RKGA) for determining the TNVE under simultaneous multi- link disruptions. The main features and benefits of the proposed method include: (a) it simultaneously solves the upper- and lower-bound problems at the same time while guaranteeing the feasibility of all solutions in the solution procedure; (b) it improves the computational efficiency to ensure the applicability to real transportation networks; and (c) it can provide a variety of alternative solutions in addition to the single optimal one, which facilitates the derivation of TNVE buffer and identification of sub-important links. These benefits make the proposed method efficient and effective for solving the TNVE problem. The applicability of the proposed method is demonstrated with small and medium-sized networks, as well as a large-scale real road network. Numerical experiments are conducted to illustrate the usage of TNVE for vulnerability analysis of transportation networks.

Keywords: Transportation network vulnerability envelope; Bi-level program; Random key genetic algorithm; Multi-link disruptions

1. Introduction

Vulnerability is an important concept for the measurement of transportation network performance under abnormal conditions, which can be defined as the network's susceptibility to disruptions, especially the severe events that can lead to failures of multiple infrastructures and significant reductions in the level of service (Berdica, 2002; Mattsson and Jenelius, 2015; Taylor, 2017; Gu et al., 2020). The evaluation of network vulnerability has been increasingly considered as an imperative topic in transportation research, which includes the tasks of measuring disruption consequences (i.e., network performance degradations) and identifying important network components (e.g., links and nodes) (Nicholson and Du, 1997; Jenelius et al., 2006; Chen et al., 2007; Qiang and Nagurney, 2008; Ryu et al., 2018; Xu et al., 2018; Esfeh et al., 2022; Gu et al., 2023). To gain a comprehensive understanding of the overall transportation network performance under severe disruptions, this study focuses on the vulnerability analysis under the simultaneous closures of multiple links. Different disruption scenarios with different severities are considered, which can facilitate the evaluation and planning of resilient transportation networks.

1.1 Review of transportation network vulnerability analysis

Transportation network vulnerability analyses are mainly conducted based on the disruption scenario enumeration approach, the game theoretic and optimization-based approach, and the approach based on sensitivity and uncertainty analysis. Table 1 briefly summarizes and classifies existing methods for transportation network vulnerability analysis. The disruption scenario enumeration is commonly used, which disrupts one link/node or simulates a disruption scenario at a time and then evaluates and ranks the impacts of different scenarios according to selected indicators. However, this approach has a combinatorial complexity to consider simultaneous disruptions of multiple links or nodes. For instance, if 10 links among 100 links
are to be simultaneously disrupted, there are over 1E+13 (C_{10}^{100}) scenarios to be evaluated. It is computationally burdensome to enumerate and evaluate all possible scenarios in practice. The sensitivity analysis-based approach addresses the combinatorial complexity by analytically computing the sensitivity of certain network performance models to minor perturbations in parameters and inputs (e.g., road capacity, travel demand, travel information). However, it is inapplicable to severe disruptions that can cause a significant reduction in infrastructure performance. The game theoretic and optimization-based approaches avoid scenario enumeration by focusing on the worst case and the most important links that can maximize performance degradation. However, only the extremely pessimistic cases are investigated in this approach, while the optimistic cases and near-extreme cases are often ignored. Owing to the difficulty of predicting the occurrence of disruptions and the likely low possibility for extreme cases to take place, merely focusing on the worst-case disruption scenarios might lead to a biased and uncomprehensive understanding of network vulnerability.

Xu et al. (2018) defined the transportation network vulnerability envelope (TNVE) to provide both the best and the worst network performances under a certain number of disrupted links. The upper and lower bounds of a TNVE can provide the possible range of network vulnerability among all disruption scenarios. Ermagun et al. (2023b) investigated the relationship between network topology and shape of TNVE, including the lower and upper vulnerability bounds and the range therebetween. Besides focusing on the single lower/upper vulnerability bounds caused by the extreme (worst and best) cases, Gu et al. (2023) further investigated the near- extreme cases that lead to sub-worst/sub-best post-disruption network performances. The TNVE buffer can then be measured, revealing the gaps between network performances in extreme and near-extreme cases. With the TNVE and its buffer, transportation network planners and managers can cost-effectively plan for system protection against disruptions and prioritize system improvements to minimize disruption risks with limited resources.

However, how to effectively evaluate the TNVE and its buffer of large-scale transportation networks under simultaneous multi-link disruptions is still an open research question. Ermagun et al. (2023a, 2023b) developed a link percolation-based approach to simulate the pessimistic and optimistic scenarios, which focuses on the sequential disruption of important links but is inadequate to reflect the extreme cases under simultaneous multi-link disruptions. Xu et al. (2018) formulated the TNVE problem as a binary integer bi-level program (BLP) model and reformulated it as a single-level mixed-integer linear program (MILP) to obtain the analytical solution. However, they mentioned that "*computational efforts required for solving MILPs are complex and difficult (i.e., solving large-scale MILPs is computationally expensive*" (Xu et al., 2018, p.351). Gu et al. (2023) further developed a single-level integer linear programming (ILP) model to derive the extreme and near-extreme cases and the TNVE buffer. Compared with Xu et al. (2018), the ILP model improves computational efficiency but requires pre-

generating a path set of the transportation network, which can become cumbersome with the increase in

network scale. In addition, the existing BLP- and ILP-based approaches derive each single extreme/near-extreme case separately. The TNVE analysis requires solving the corresponding model multiple times under each number of disrupted links, which further increases the computational burden when many links are to be disrupted in large-scale networks.

Table 1. Classification of existing transportation network vulnerability analysis

Category	**References**	**Logic**	**Limitations**
Disruption scenario enumeration approach (enumeration w/o or with pre-scan, or random simulation)	Chen et al., (2007); Qiang and Nagurney (2008); Jansuwan and Chen (2015). Reviewed by Mattsson and Jenelius (2015)	One link/node is removed at a time, and the impact of each link/nodal removal is evaluated and ranked according to different indicators	Inapplicable to consider simultaneous disruptions of multiple links/nodes owing to the combinatorial complexity of enumerating all possible combinations of disrupted links/nodes
Sensitivity and uncertainty analyses	Nicholson and Du (1997); Yang and Chen (2009); Luathep et al., (2011); Connors and Watling, (2015); Du et al., (2022); Gu et al., (2022)	Link importance is the proportion of overall uncertainty of performance measure contributed by its link capacity uncertainty	Only valid for minor perturbations; inapplicable to large perturbations (e.g., link closure) in extreme disruption scenarios
Game theoretic and optimization-based approach	Bell (2000); Bell et al. (2008); Szeto (2011) Wang et al., (2016); Szymula and Bešinović (2020)	Important links are likely to be destroyed by the demon as a consequence of the game	Only consider the worst-case scenario (i.e., pessimistic evaluation); inadequate to reveal network performances in more general disruption scenarios
Vulnerability envelope analysis	Xu et al., (2018); Ermagun et al., (2023a, 2023b); Gu et al., (2023)	Identify important and sub-important link combinations, derive corresponding vulnerability bounds and buffers and vulnerability range therebetween	Need to derive each extreme/near-extreme case separately. The derivation of TNVE either fails to cover all possible disruption scenarios (Ermagun et al., 2023a, 2023b), or requires a high computational effort (Xu et al., 2018), or pre-generation of path sets (Gu et al., 2023)

1.2 A brief review of random key genetic algorithm

In this study, we develop a method based on the random key genetic algorithm (RKGA) to efficiently solve the BLP-based TNVE model. Genetic algorithm (GA) is one of the well-known evolutionary computing techniques (see Goldberg and Holland, 1988; Gen and Cheng, 1999 for a detailed description of GA), which makes use of the biological evolution procedure

for the update of decision variables (genes) and solutions (chromosomes). GA has been successfully applied to solving a variety of complex transportation problems, such as vehicle routing (Karakatič, 2021; Hien et al., 2022), path-finding under uncertainty (Ji et al., 2011; Rajabi-Bahaabadi et al., 2015), path planning (Nunes et al., 2023; Paulavičius et al., 2023), road maintenance (Chootinan et al., 2006; Altarabsheh et al., 2023), traffic counting location (Chootinan et al., 2005; Sun et al., 2021), network design (Chen et al., 2006, 2010a; Chen and Xu, 2012; Salman and Alaswad, 2022; Zhou et al., 2023; Ziar et al., 2023), and network evaluation and optimization under disruptions (Li et al., 2019; Huang et al., 2021; Liu et al., 2022). However, the traditional GA is not directly suitable for the TNVE problem due to the difficulty of guaranteeing solution feasibility in the evolution process. This issue can be addressed by the RKGA proposed by Bean (1994), where a random key-based representation of a solution was introduced to maintain feasibility for each new solution. The RKGA and its extension, biased RKGA (Gonçalves and Resende, 2011; Andrade et al., 2021), has been widely applied to many classic optimization problems associated with transportation research, including the traveling salesman problem (Snyder and Daskin, 2006; Samanlioglu et al., 2008; Ruiz et al.,2019), scheduling problem (Mendes et al., 2009; Zhou et al., 2018; Andrade et al., 2019; Xie et al., 2022), and facility location problem (Biajoli et al., 2019; Londe et al., 2021; De Freitas et al., 2023).

1.3 Contributions and organization

Benefiting from the RKGA, the proposed method contributes to the TNVE analysis in the following aspects:

(a) The proposed method can reduce the computational requirement posed by the bi-level nature of the BLP-based TNVE model while guaranteeing solution feasibility. Furthermore, it can enhance computational efficiency by deriving both lower and upper vulnerability bounds together. Thus, the applicability of the TNVE analysis to large-scale real-world transportation networks is ensured.
(b) The proposed method generates a population of feasible and near-optimal solutions, which enables the simultaneous evaluation of both extreme and near-extreme cases under simultaneous multi-link disruptions, which can be used to identify sub-important link combinations and measure TNVE buffers.
(c) With the help of the proposed method, the TNVEs of different sizes of transportation networks are investigated. The slopes of vulnerability bounds, range between the two bounds, and the near-extreme disruption scenarios with corresponding envelope buffers are examined, which can provide insights into the understanding and analysis of TNVE.

The remainder of this paper is organized as follows. Section 2 presents and explains the BLP-based TNVE model, followed by the RKGA-based method to solve it in Section 3. Numerical experiments are carried out to illustrate the effectiveness, efficiency and applicability of the proposed method based on networks of different sizes in Section 4. Section 5 concludes the paper and provides some directions for future studies.

2. Bi-level vulnerability envelope model

This section presents the formulation and interpretation of the BLP-based TNVE model, which aims to maximize/minimize the network performance under simultaneous disruption of multiple links. Thus, by deriving the solutions to the maximization/minimization BLP models, one can obtain the upper/lower bounds of TNVE and identify corresponding important links.

The BLP model can circumvent the enumeration of all possible disruption scenarios and obviate the need of path set pre-generation in the studied transportation network.

2.1 Notations

Sets

A	Set of links.
W	Set of O-D pairs.
O_i	Set of links emanating from node i
I_i	Set of links going into node i

Parameters

t_a	Travel cost of link a.
u^w	Post-disruption travel cost between O-D pair w.
u_0^w	Reference travel cost between O-D pair w.
θ	Allowable elongation ratio of accepting a detoured route relative to a reference cost u_0^w.
n	Number of disrupted links.
ε	A sufficiently small positive constant.
M	A sufficiently large positive constant.

Decision variables

x_a	Binary variable indicating whether link a is disrupted. $x_a = 1$ when a is disrupted; otherwise, $x_a = 0$.
y_a	Binary variable indicating whether link a is used in the minimum cost route. $y_a = 1$ when a is used; otherwise, $y_a = 0$.
z^w	Binary variable indicating whether O-D pair w is connected. $z^w = 1$ when w is connected; otherwise, $z^w = 0$.

2.2 Upper-level model

The upper-level model aims to find the upper/lower bound of TNVE (i.e., the maximum/minimum network performance) under a given number of disrupted links n, which is formulated as the following binary integer linear program (Xu et al., 2018):

$$\max_{\mathbf{z}} f(\mathbf{x}, \mathbf{z}) = \sum_{w \in W} \quad \text{(Upper-bound problem)} \tag{1-1}$$

$$\min_{\mathbf{z}} f(\mathbf{x}, \mathbf{z}) = \sum_{w \in W} \quad \text{(Lower-bound problem)} \tag{1-2}$$

s.t.

$$\sum_{a \in A} x_a = n \tag{2}$$

$$-Mz^w + \varepsilon \le u^w - \theta_0 u^w \le M(1 - z^w), \quad \forall w \in W \tag{3}$$

$$xa = \{0, 1\}, \quad \forall a \in A \tag{4}$$

$$zw = \{0, 1\}, \quad \forall w \in W \tag{5}$$

where $|A|$ is the size of set A (i.e., the number of links). The objective functions in Eq. (1-1) and Eq. (1-2) are to **Error! Reference source not found.**maximize and minimize the remaining network connectivity after disrupting n links. Eq. (2) is the cardinality constraint imposed on the total number of disrupted links. Constraint (3) is the linkage constraint between the upper- and lower-level models, where the decision variable z^w is determined based on the variable u^w obtained from the lower-level model. θ (>1) denotes the travelers' allowable elongation ratio, i.e., the acceptable ratio of a post-disruption O-D travel cost relative to a reference cost u_0^w (e.g., the shortest path travel cost between O-D pair w in a normal situation). When θ approaches positive infinity, only the physical connectivity is considered, i.e., travelers can accept all physically connected routes between each O-D pair disregarding the length of detour; when θ approaches 1, it implies a high requirement on the level of service, i.e., travelers accept only the shortest path with no detour. Eq. (4) and Eq. (5) state that the decision variables are binary integers. If link a is disrupted, x_a = 1, and 0 otherwise; and if O-D pair w is connected, z^w = 1, and 0 otherwise.

2.3 Lower-level model

The lower-level model aims to obtain the post-disruption O-D travel cost based on the link disruption scenario (i.e., values of decision variable x_a) determined at the upper level, which can be considered as a virtual link cost-based shortest path problem and be formulated as the following linear program (Xu et al., 2018):

$$\min_{\mathbf{y}} uw = \sum_{a\in A} \left(t_a y_a + M \cdot x_a y_a\right) \tag{6}$$

s.t.

$$\sum_{a\in O_i} y_a - \sum_{a\in I_i} y_a = \begin{cases} 1, & \text{if } i = r \\ -1, & \text{if } i = s \\ 0, & \text{otherwise} \end{cases} \tag{7}$$

$$y_a \geq 0, \quad \forall a \in A \tag{8}$$

where r denotes an origin, and s denotes a destination. Eq. (6) minimizes the total travel cost of the selected links for each O-D pair. A virtual cost M is imposed to indicate the consequence of link disruptions, making the objective function different from the classical shortest path problem. If link a is disrupted (i.e., x_a = 1), its virtual link cost is $t_a + M$; otherwise, its cost remains as t_a. Eq. (7) is the node conservation constraint based on the binary variable y_a (y_a =1 if link a is used in the shortest path, and 0 otherwise).

2.4 Interpretations of vulnerability envelope

The TNVE provides decision-makers with the upper and lower bounds of network vulnerability and the range therebetween, which are useful in the design of network protection strategies and prioritization of system component improvements. Particularly, the links that repeatedly appear in the lower-bound scenarios under different numbers of disrupted links might deserve more resources and actions to protect or reinforce in the pre-disruption network planning stage. Figure 1 exemplifies the TNVEs derived based on four

transportation networks with different

topologies. The interpretations of TNVE are demonstrated as follows:

(1) The locations of both bounds indicate the overall network vulnerability under multi-link disruptions. For example, networks (a) and (d) have similar curves of the lower bound with network (c) but much higher curves of the upper bound. This implies networks (a) and (d) might be less vulnerable than network (c) as they have similar performance under pessimistic situations but are possible to outperform network (c) under optimistic situations.

(2) The slope of vulnerability bounds indicates the sensitivity of network performance with respect to the disruption severities (number of disrupted links). A large slope (i.e., a steep decrease) of the upper bounds of networks (a) and (d) after a small number of disrupted links implies the corresponding range of disruption severity is critical to the network performance under the best-case disruption scenarios.

(3) The range between upper and lower bounds implies the uncertainty of network performance under a certain number of disrupted links. For instance, network (c) has a similar shape of the TNVE with network (b) but a larger vulnerability range, implying larger possible variations in network performance under different disruptions.

Overall, these interpretations help us to evaluate the performance of the network and serve as a guide for decision-making.

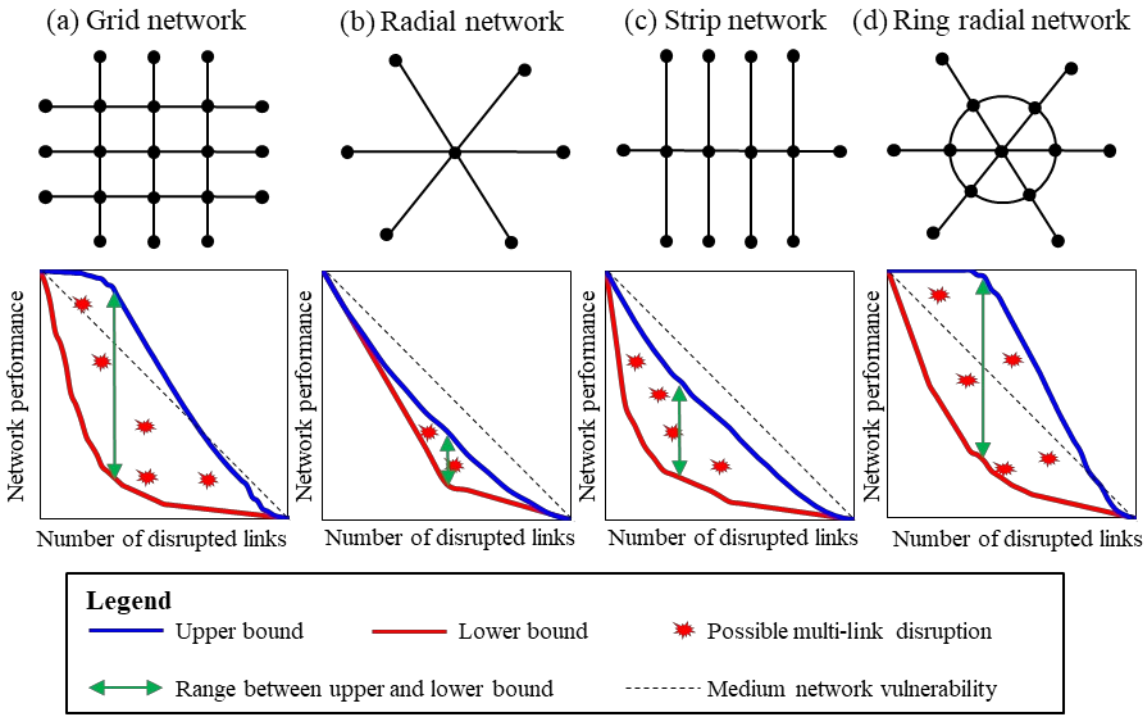

Figure 1. Interpretation of TNVE

3. RKGA-based vulnerability envelope derivation

The abovementioned BLP model imposes a high computational burden to obtain exact solutions, which can become intractable when applied to large-scale networks (Xu et al., 2018). It is necessary to develop effective algorithms to improve computational efficiency. In this section, a heuristic method based on the RKGA is developed for solving the BLP-based TNVE model, which can simultaneously derive both upper and lower vulnerability bounds, as well as their buffers and corresponding sub-important links.

3.1 Preliminaries on GA and RKGA

The GA is an efficient metaheuristic widely adopted to solve combinatorial optimization problems, which generates and evolves a large population of solutions inspired by the process of biological evolution. The traditional GA consists of the encoding and decoding of chromosomes (solutions to the model) and operators for evolving chromosomes, including reproduction, crossover, and mutation. First, a chromosome is encoded as a list of genes, which are digits representing the valuation of each decision variable in the solution. An initial population of chromosomes is then randomly generated for further iterations. At each iteration, a new population is generated including chromosomes from three operators: (1) the elite chromosomes (with the best fitness values) directly copied from the last iteration (reproduction), (2) the offspring chromosomes as a combination of genes from two parent chromosomes at the last iteration (crossover), and (3) the offspring chromosomes with most of the genes inherited from parent chromosomes but a few genes generated randomly (mutation). The reproduction operator maintains good solutions obtained in the evolution process, while the crossover and mutation operators can improve solutions by manipulating good genes and enhance population diversity by adding new genes to the population.

However, the traditional GA cannot be directly applied to solve the TNVE problem owing to its inadequacy to handle the cardinality constraint (Eq. (2)). For the TNVE problem, decision variables (x_a) are represented by a binary integer string. Each gene has a value of either 0 or 1, which indicates the disruption of link a. Consider a network with n=3 and five potential disrupted links (i.e., $|A|$=5). Figure 2 shows an example of two parent chromosomes that are directly encoded based on the values of decision variables x_a, and their offspring chromosomes generated by crossover. The crossover of parents a and b can lead to the violation of cardinality constraint (the numbers of disrupted links are respectively n=2 and n=4 in the two offspring chromosomes), and hence generates infeasible solutions.

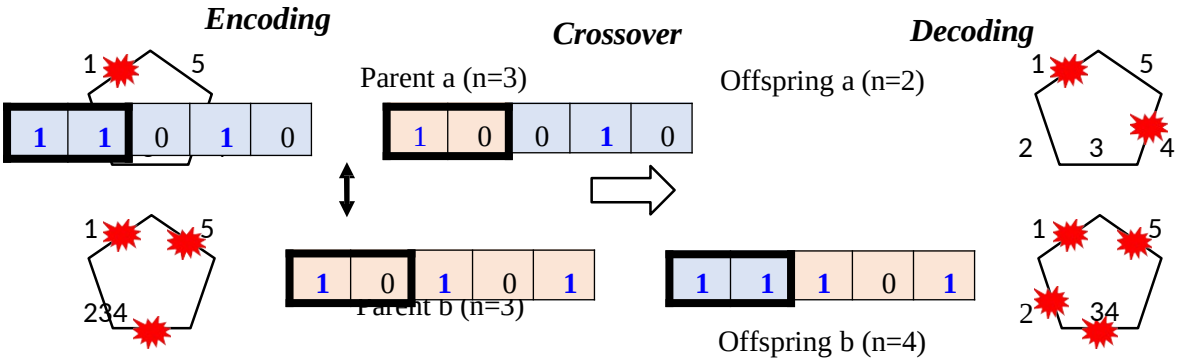

Figure 2. An example of chromosomal encoding and crossover of traditional GA

To address the infeasibility issue, this study develops an RKGA-based method for the TNVE problem, where random keys are introduced in the encoding of chromosomes (Bean, 1994). In the encoding of chromosomes, random keys instead of binary integers are used. A simple ordering method is presented to decode the solution from encoded random numbers, which can guarantee the feasibility of the cardinality constraint. Compared with the traditional GA operators (i.e., reproduction-crossover-mutation), we adopt the biased crossover from the biased RKGA, which allows us to mate between elite and non-elite chromosomes for

generating the offspring. Additionally, instead of the mutation step that introduces new genes into existing chromosomes, an immigration step is adopted to introduce new chromosomes, which adds more diversity to the population.

Figure 3 shows the overall framework of the RKGA-based method. An initial population is first generated and encoded, which is then updated by the RKGA operators for solving the upper- and lower-bound problems in parallel. The detailed steps of chromosomal encoding and each RKGA operator will be illustrated in Sections 3.2 and 3.3. The obtained optimal solutions with the lowest and highest objective values construct the upper and lower vulnerability bounds. Alternative near-optimal solutions can also be obtained to construct the TNVE buffer, which indicates the gaps between extreme and near-extreme disruption scenarios.

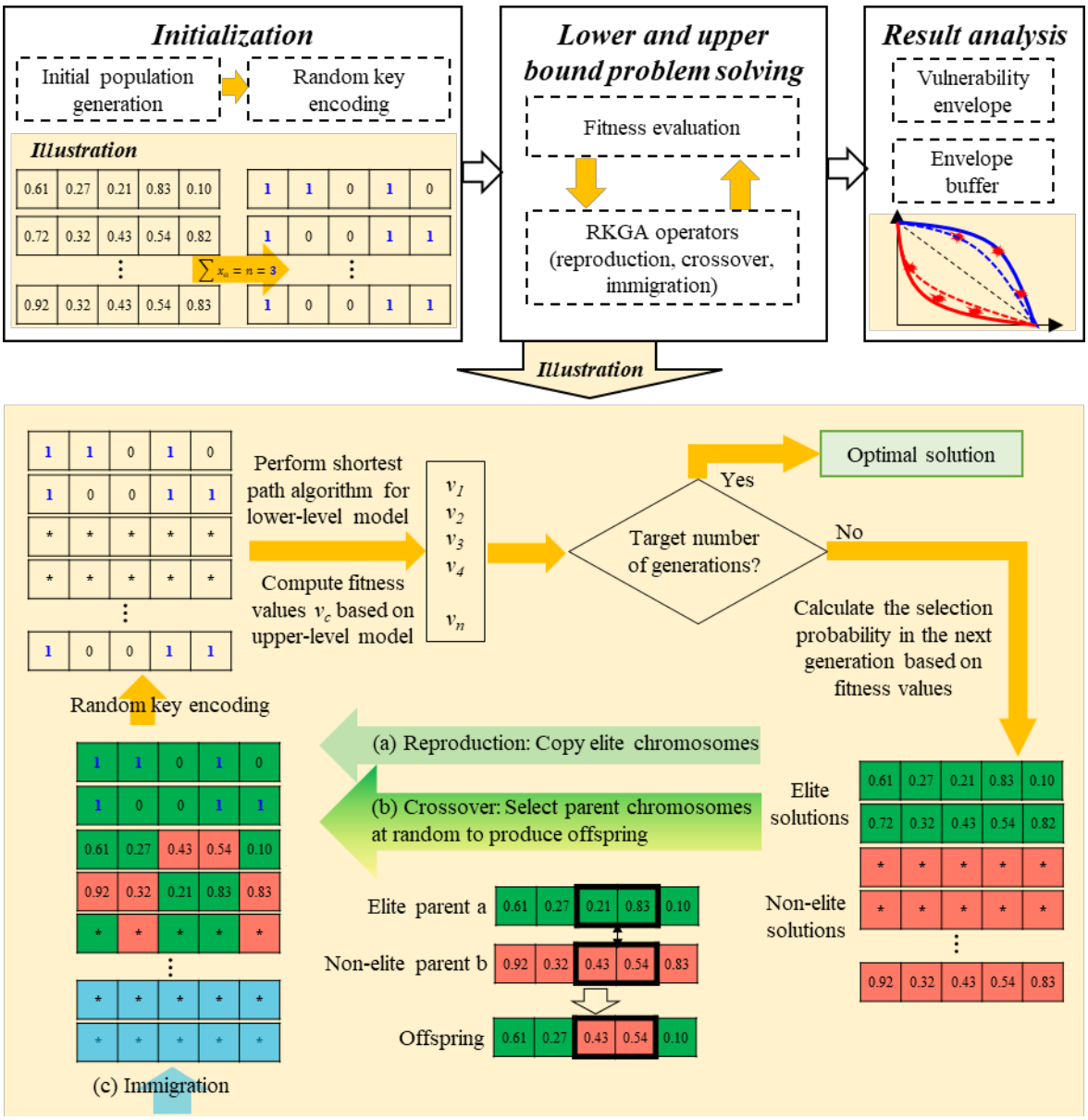

Figure 3. Overall framework of the RKGA-based method for TNVE problem

3.2 Random keys chromosomal encoding

To generate an initial population, a random key (a random real number sampled from [0,1][1]) is generated for each gene in a chromosome, and each gene can be decoded as a binary integer based on the ordering of random keys. Figure 4 shows an example of encoding based on the same network considered in Figure 2 (i.e., $|A|$=5 potential disrupted links). In the decoding, the link with a larger random key has a higher priority to be disrupted. Under the three-link disruption scenario (n=3), the three genes with the largest random numbers (i.e., links 1, 2, 4) are decoded as disrupted links (x_a=1), while the other genes are decoded as undisrupted links (x_a=0). While under the four-link disruption scenario (n=4), links 1, 2, 3, 4 are selected as disrupted links. Thus, the decoding procedure of chromosome generation naturally handles the cardinality constraint on the number of disrupted links (Eq. (2)) and ensures solution feasibility.

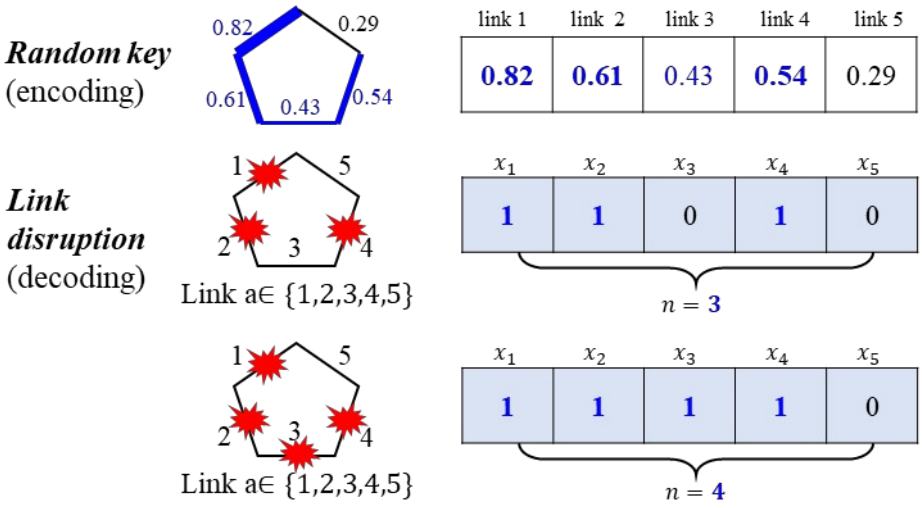

Figure 2. Example of random keys chromosomal encoding

3.3 RKGA Operators

RKGA operators, which are reproduction, crossover, and immigration, will be applied to maintain good solutions and introduce new solutions. These three operators generate a new population at each iteration until the stopping criteria are met (e.g., the maximum number of generations). The RKGA operators used in this study are described below.

3.3.1 Reproduction

Reproduction is a process of selecting solutions (i.e., parents) from a pool of populations for mating purposes within the feasible region. It directs the genetic search toward the promising area of the search space. The solutions are selected based on their fitness value. The fitness value of solution c (v_c) is computed as follows:

$$v_c = \sum_{\substack{(\mathbf{x}) \\ c \in P}} z_c \tag{9}$$

[1] In this paper, the random keys are randomly drawn from a uniform distribution over the interval [0,1] via the "numpy.random.uniform" component in Python.

where P is the population; **x** denotes the vector of x_a^c, which indicates whether link a is disrupted on chromosome c. z_c is the objective value derived based on the decision variables x_a^c carried by solution c. Once the link disruption pattern **x** is given, the virtual link cost used in Eq. (6) is fixed, and hence the lower-level model can be efficiently solved by existing shortest path algorithms. The corresponding objective value z_c can then be evaluated based on the shortest path travel time between each O-D pair obtained at the lower level. Based on the ranking of fitness values, the solutions are grouped into elite and non-elite populations. The elite chromosomes are copied to the next generation in the reproduction step.

3.3.2 Crossover

The crossover operator provides the means to stochastically manipulate the existing solutions to generate new offspring. The developed method adopts the biased crossover used in the biased RKGA, which crosses between elite and non-elite populations. Here, we use the roulette wheel selection to randomly select the candidate solution from each population. The solution with a better fitness value (i.e., a higher/lower value in the upper-bound/lower-bound problem) will occupy a larger portion on the roulette wheel and have a larger probability to be selected. The selection process is based on a random number drawn between 0 and 1 (similar to spinning the roulette wheel) and the solution associated with the intercepted portion of the wheel will enter the mating pool. The chance for an individual solution to be selected (or probability of survival) is determined based on the distance measure within the corresponding population:

$$\Phi_c^{\min \text{ or } \max} = \frac{\left| v_c - v_{\min \text{ or } \max} \right|}{\sum_c \left| v_c - v_{\min \text{ or } \max} \right|}, \tag{10}$$

where v_{min} and v_{max} are the minimum and maximum fitness values in the corresponding group, which are respectively used in the upper- and lower-bound problems. In this way, the new offspring inherit characteristics from both populations.

Genetic materials may be exchanged at different points along the chromosomes. The crossover operator can be a one-point crossover or a slightly complicated multi-point crossover. In this study, we use the uniform crossover in which the exchanges of genetic materials occur at the points corresponding to the crossover mask. The crossover mask is a list of binary variables with the same length as the chromosome, which indicates whether the parent chromosome supplies genetic units to the offspring. For example, the offspring resembles the characteristics of the elite chromosome if the value of the corresponding mask is 1, or the characteristics of the non-elite chromosome otherwise. In this study, we use the probability of 70% to generate crossover mask 1, which means that the offspring resembles 70% of the characteristics of the elite parent and 30% characteristics of the non-elite parent. The crossover operator is illustrated in Figure 5.

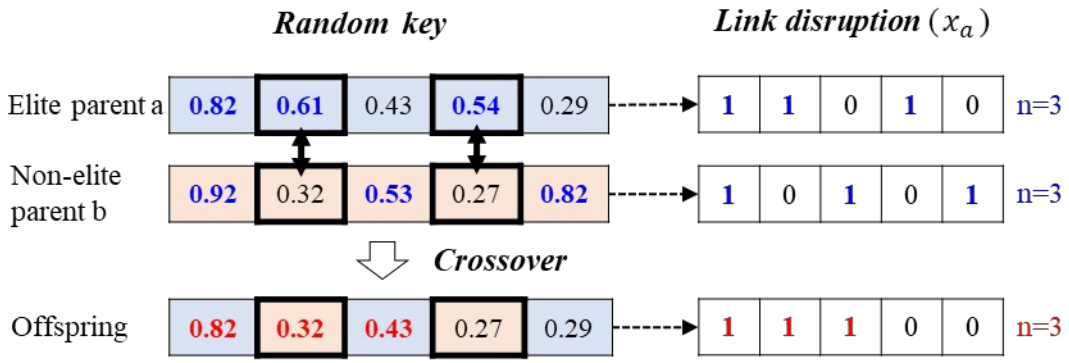

Figure 5. Illustration of crossover operator

3.3.3 Immigration

The traditional GA includes a mutation operator to introduce new genes into the chromosome pool, which provides an ability to jump out of the local optima whenever it is getting trapped. However, the probability of introducing new genes is small based on the mutation operator that randomly changes some genes in the existing chromosome. In RKGA, the immigration operator shown in Figure 6 is adopted to generate a more diverse population. The immigration operator randomly generates a small proportion of new chromosomes following the same technique of generating the initial population, which brings higher diversity. In summary, the population in the new generation is comprised of the elite solutions copied in the reproduction operator, the offspring solutions obtained in the crossover operator, and the new solutions generated in the immigration operator.

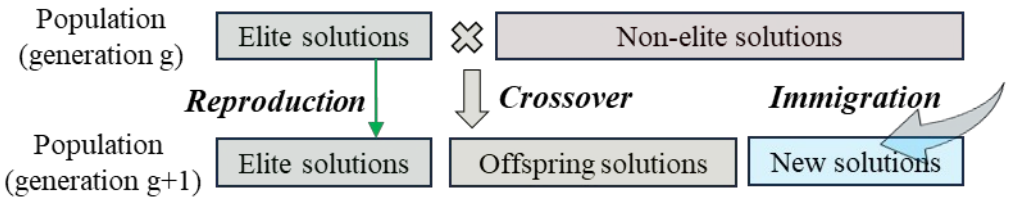

Figure 6. Illustration of immigration operator

4. Numerical results

To demonstrate the proposed RKGA-based method for solving the TNVE problem, experiments are conducted based on three networks for different purposes. The proposed method is coded using Python and runs on a personal computer with an INTEL® Core (TM) i7-6700@3.40GHz CPU and 16GB RAM with Windows 10 operating system. First, a small network is used to verify the effectiveness of the proposed algorithm and to analyze the convergence performances with respect to algorithm parameters. Then, a medium-size network is employed to illustrate the evaluation of TNVE based on the upper and lower vulnerability bounds and the vulnerability range therebetween. Finally, the applicability to large-scale transportation networks is demonstrated based on the network in Winnipeg, Canada. The ability of the proposed method to identify sub-important link combinations and analyze TNVE buffer is also shown via the experiment on the Winnipeg network.

4.1 Small network

The toy network shown in Figure 7 consists of 6 nodes, and 16 directed links (Xu et al., 2018). There are 14 O-D pairs consisting of (1, 2), (1, 3), (1, 4), (2, 1), (2, 3), (2, 4), (3, 1), (3, 2), (3,
4), (4, 1), (4, 2), (4, 3), (5, 6), and (6, 5). The population size is set as 32. The uniform crossover with a crossover rate of 0.7 is adopted. A 10% immigration rate and a 10% reproduction rate are used. The elongation ratio θ is set as a sufficiently large positive constant, indicating that in this section, the TNVE analysis considers the physical connectivity of each O-D pair disregarding the length of detour under disruption.

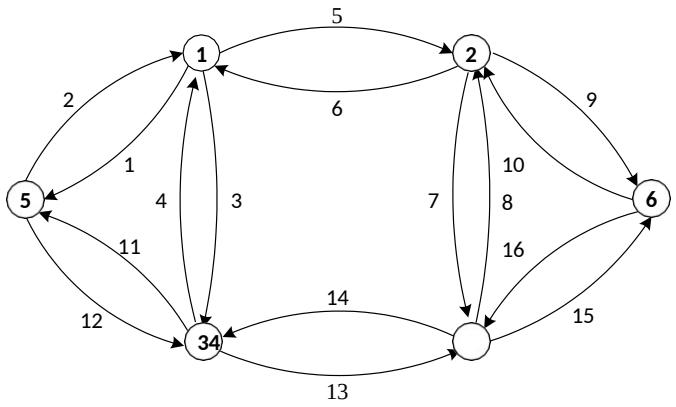

Figure 7. Toy network (adapted from Xu et al., 2018)

4.1.1 Vulnerability envelope

Figure 8 shows the upper and lower vulnerability bounds and the identified important link combinations under each number of disrupted links (n). The results show that the proposed method can replicate the exact solutions obtained via the analytical solution procedure from Xu et al. (2018). Specifically, the resulting TNVE is exactly consistent with that obtained under the complete path set, which is more optimistic (i.e., has higher lower and upper vulnerability bounds) than the TNVE derived under a more restrictive path set (Gu et al., 2023). However, the analytical solution method developed by Xu et al. (2018) requires higher computational efforts and needs to separately solve the upper- and lower-bound problems (i.e., solve the TNVE model two times: one for the maximization problem and another for the minimization problem). On the other hand, the single-level ILP-based vulnerability envelope model developed by Gu et al. (2023) requires a pre-generation path set, which can be cumbersome in large-scale networks. The proposed method is more computationally efficient and can simultaneously determine both upper and lower bounds at the same time without a priori path set information. For more analysis of the resulting TNVEs under different path sets, readers are referred to Xu et al. (2018) and Gu et al. (2023).

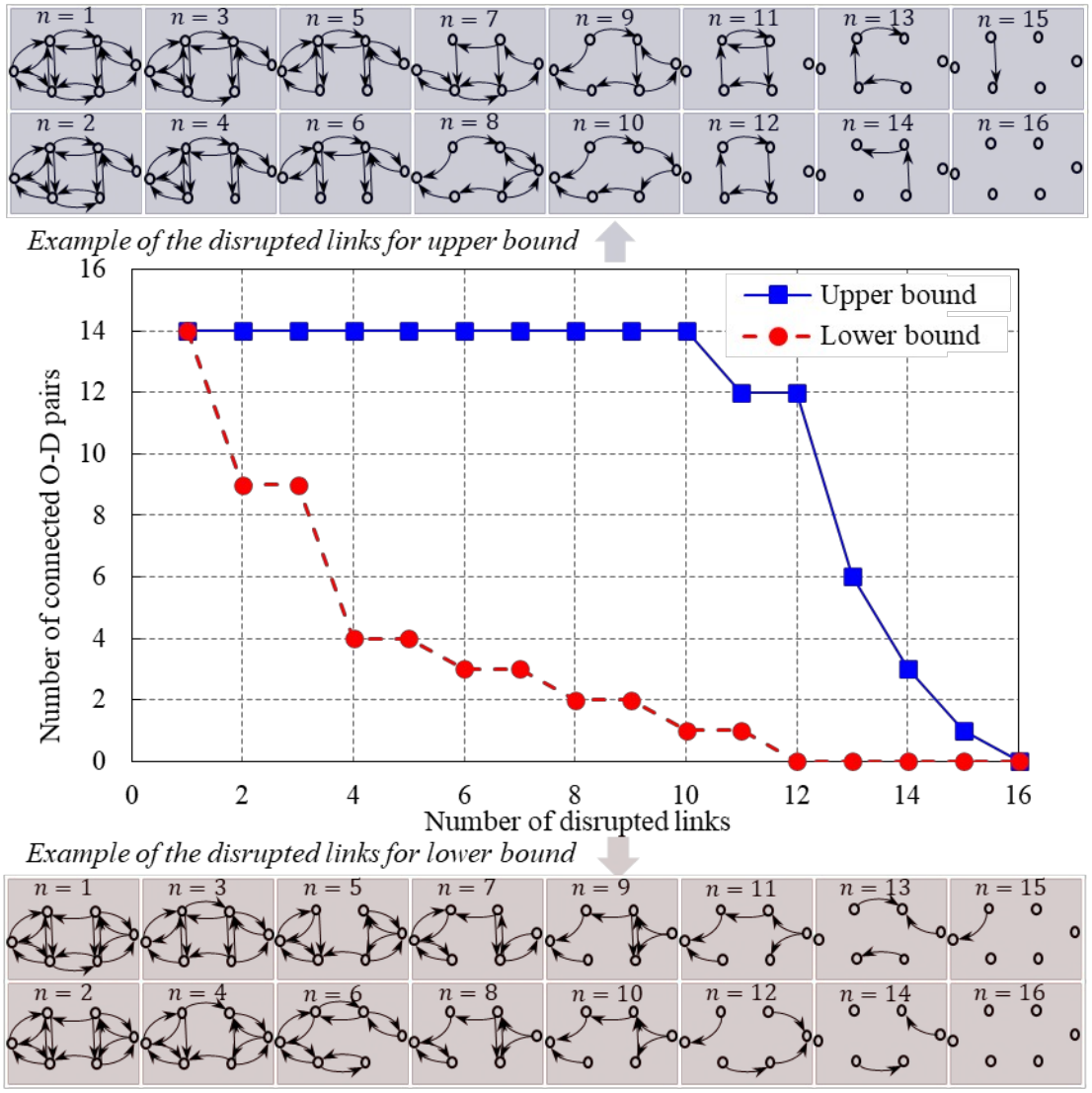

Figure 8. TNVE with disrupted links for both upper and lower bounds of the small network

4.1.2 Convergence performance with respect to algorithm parameters

In this section, we analyze the sensitivity of convergence performance of the proposed method with respect to the population size and number of generations. Six different cases, including three lower-bound problems (termed LB) and three upper-bound problems (termed UB), are selected for the sensitivity analysis with respect to the population size. 1,000 generations with 100 trials for each generation are used in the experiment. Figure 9(a) shows the average number of iterations to reach the convergence when the population size varies from 8 to 256. In all cases, a larger size of population requires fewer iterations for convergence. From the comparison among different cases, the upper-bound problem tends to converge slower than the lower-bound problem. The number of disrupted links also has a significant impact on the convergence speed. When the number of disrupted links increases from 2 to 6, the number of possible link combinations dramatically increases. Thus, a much larger number of iterations are required to solve the corresponding lower-bound problem. Similarly, when the number of disrupted links increases from 10 to 13, the combinatorial complexity decreases, leading to a significant decrease in the number of converged iterations required by the corresponding upper- bound problem.

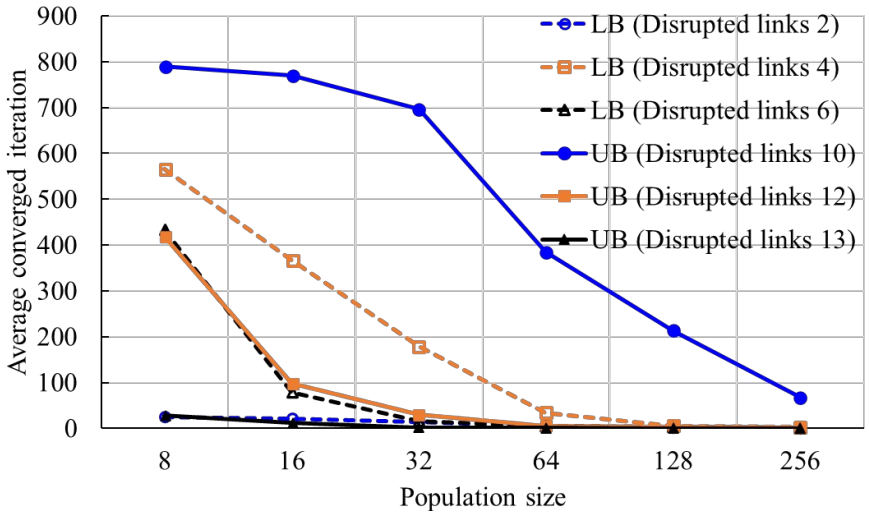

(a) Average number of converged iterations with varying population sizes

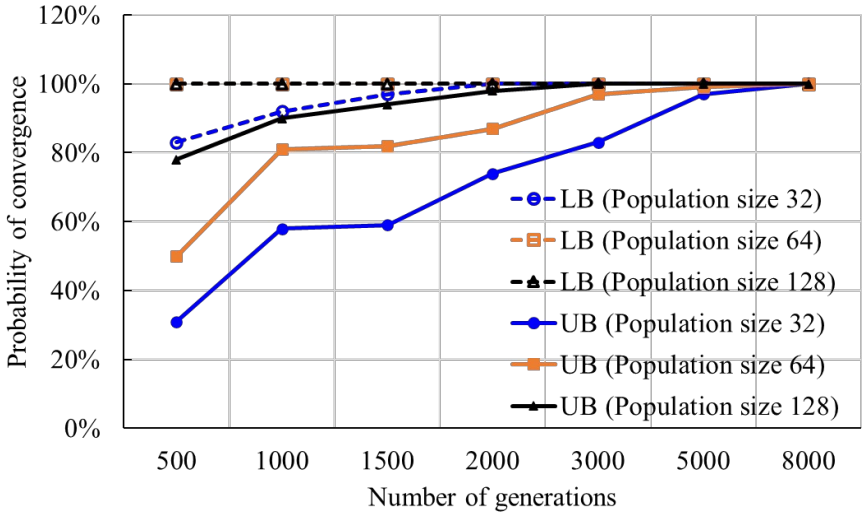

(b) Probability of reaching convergence after 100 trials with varying numbers of generations

Figure 9. Convergence performance with respect to algorithm parameters

Figure 9(b) shows the percentage of convergence in 100 trials under varying numbers of generations. In this experiment, 4-link disruption and 10-link disruption, which have the same combinatorial complexity, are respectively examined in the lower- and upper-bound problems. The vertical axis indicates the convergence probability. For example, 83% indicate that the optimal solutions are found 83 times among 100 trials. The observed convergence percentage is unsatisfactory when a small population or fewer generations is used. The convergence becomes more likely with the increase in population size and number of generations and can be guaranteed when the population size reaches 128 or the number of generations reaches 5,000.

4.2 Medium network

The Sioux Falls network shown in Figure 10(a) is a widely adopted network to test various transportation models, including those focusing on the network evaluation and optimization under disruptions (Xu et al., 2021). Successfully applying the RKGA method in the Sioux Falls network verifies its higher computational efficiency and applicability than the exact method developed by Xu et al. (2018). There are 24 nodes, 76 directed links, and 552 O-D

pairs in the

network. In this experiment, we set the population size as 2,048 and the number of generations as 2,000. The elongation ratio parameter θ is set to 1.5. We consider pairwise link disruptions, where one road disruption indicates the closures of bi-directional links (e.g., the disruption of the road between nodes 1 and 2 indicates the simultaneous closures of links 1 and 3).

The upper and lower vulnerability bounds obtained from the proposed method are shown in Figure 10(b). Note that there is a total of 7.55E+22 possible combinations, and hence it is computationally difficult to find vulnerability bounds via the analytical method. From Figure 10(b), the lower bound has a steep decrease from n = 1 to n = 8. In this segment of disruption severity, disrupting one more road can lead to the disconnections of 45 O-D pairs in the worst case. On the other hand, the severity segment from n = 14 to n = 26 witnesses a steep decrease in the upper bound, in which 24 O-D pairs become disconnected under the disruption of one more road. The largest slope of the lower bound occurs at n = 4. Compared to the worst case under 3-link disruption, the worst case of 4-link disruption can disconnect 72 more O-D pairs. n = 20 is a critical point in the upper-bound problem, where 30 more O-D pairs become disconnected compared to n = 19. This implies that more attention should be paid to the reinforcement and protection of important links identified under critical disruption severities, where the transportation network is more sensitive to the severity of multi-link disruptions.

Figure 10(c) investigates the vulnerability range, i.e., the difference between upper and lower bounds under each disruption severity, which implies the uncertainty in network vulnerability (Ermagun et al., 2023b). The largest vulnerability range is 357 from n = 10 to n = 14. In this section, the network may perform distinctly in pessimistic and optimistic cases, implying a high variation in the network performance in different disruption scenarios. The decision-makers are suggested to treat these disruption severities with caution and avoid biased network performance evaluation by considering both pessimistic and optimistic cases.

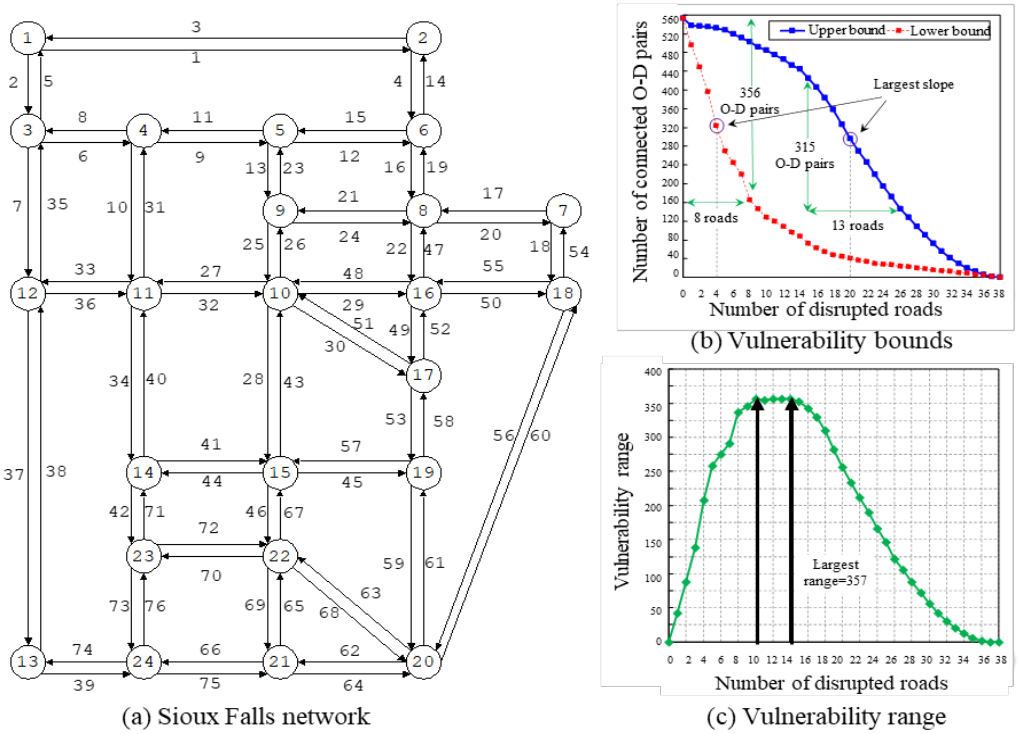

(a) Sioux Falls network

(b) Vulnerability bounds

(c) Vulnerability range

Figure 10. Sioux Falls network topology and the corresponding vulnerability bounds and vulnerability range

4.3 Winnipeg network

In this section, we assess the vulnerability under bridge disruptions in the city of Winnipeg, Manitoba, Canada. The urban road network is shown in Figure 11, which consists of 154 zones, 1,067 nodes, 2,535 links, and 4,345 O-D pairs. There are 15 major bridges spatially located for crossing the Red River (eastbound– westbound direction) and the Assiniboine River (northbound–southbound direction). The rivers divide the city into three major regions, implying the importance of bridges in road network connectivity. Region 2 includes the central business district (CBD) area and has relatively more O-D pairs. Region 1 is a larger area than region 3 with more O-D pairs (see Table 2). We classify the 15 bridges into three groups based on their role in network connectivity: group A (A1-A5) connecting regions 1 and 2; group B (B1 to B4) connecting region 1 and 3; and group C (C1 to C6) connecting region 2 and 3. The algorithm parameters are set as follows: the population size is 512, the number of generations is 500, the crossover rate is 0.7, a 10% immigration rate and a 10% reproduction rate are used. The elongation ratio parameter (θ) is set as 2.0, i.e., the analysis considers travelers to accept two times as long as their shortest path.

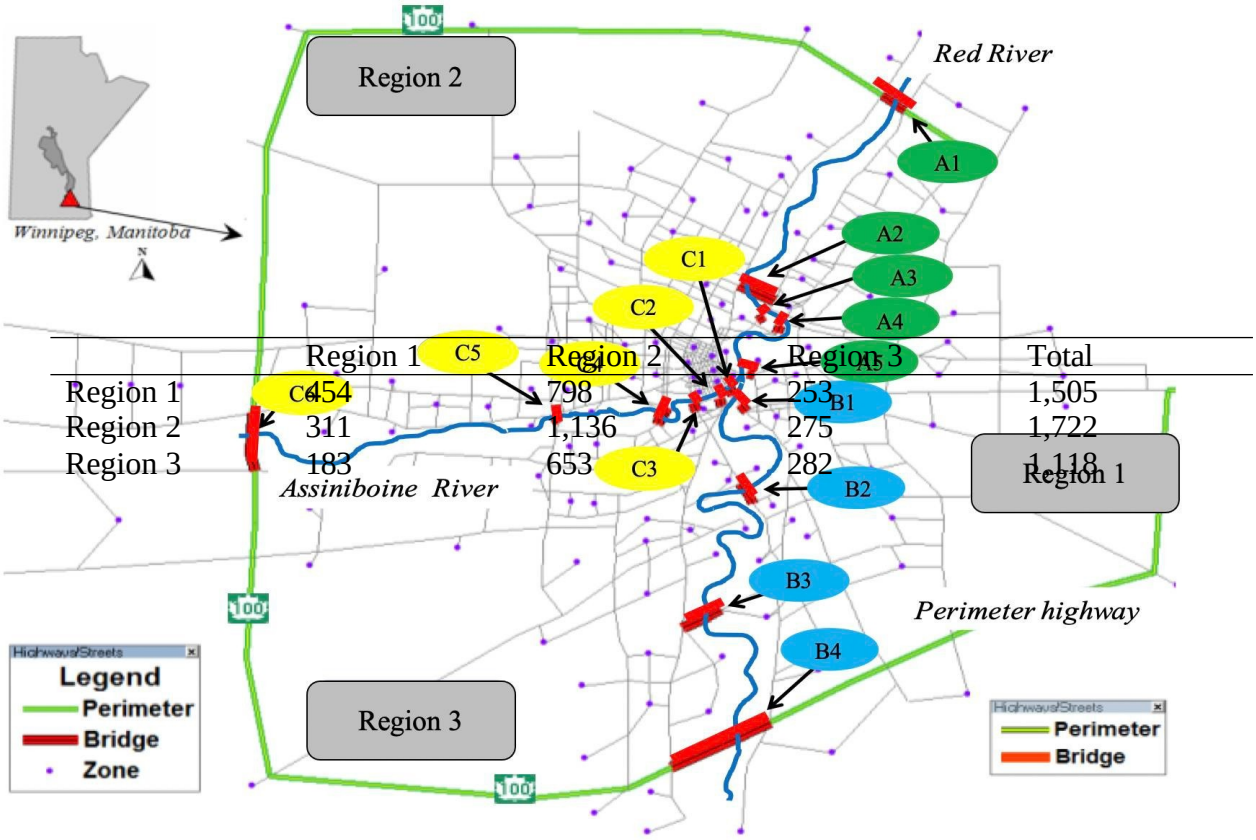

Figure 11. Locations of 15 bridges in the Winnipeg network

Table 2. Number of O-D pairs between regions

	Region 1	Region 2	Region 3	Total
Region 1	454	798	253	1,505
Region 2	311	1,136	275	1,722
Region 3	183	653	282	1,118

Total	2,587	810	948	4,345

4.3.1 Vulnerability envelope

The optimal solutions to upper- and lower-bound models obtained from the RKGA method are shown in Figure 12. Compared with the TNVE of the Winnipeg network derived by Gu et al. (2023), the TNVE from the RKGA method is much more optimistic given its relatively higher upper/lower bounds with flatter slopes. This can be attributed to the complete path set considered by the proposed method, which is more optimistic than the behaviorally generated path set considered by Gu et al. (2023). While it is computationally burdensome to enumerate a path set for applying the single-level ILP-based vulnerability envelope model (Gu et al., 2023), the RKGA method inherently avoids the path set generation process by solving the lower-level shortest path problem. The complete path set embedded in the RKGA method is beneficial for vulnerability assessment under various extreme disruptive events, in which the most important task is to retain connected paths between each O-D pair, even though the paths might not be frequently used in normal conditions.

In the TNVE, the lower bound steeply decreases from n = 5 to n = 11, whereas the upper bound has a quick decrease from n = 14 to n = 15. In the severity segment from n = 1 to n = 11, disrupting one more road averagely leads to disconnections of 185 O-D pairs in the worst case. As for the upper bound, from n = 14 to n = 15, an average of 1,160 O-D pairs are disconnected due to one more road disruption. The largest slope of the lower bound occurs at n = 9, where 545 more O-D pairs become disconnected compared with n = 8. n = 14 is a critical point in the upper bound, at which 1,255 more O-D pairs are disconnected compared with n = 13. The largest range between lower and upper bounds is 1,999, which occurs at n = 11.

Figure 12 also shows the disrupted bridges on the upper and lower bounds. In the upper-bound problem, at least one bridge in each bridge group remains intact, which enables the connections of most O-D pairs. Under the 13-bridge disruption, all bridges in group B are disrupted, making many O-D pairs from region 1 to region 3 disconnected. When n = 14, all bridges in groups B and C are disrupted, thus O-D pairs related to region 3 (the region disclosed by bridge groups B and C) are disconnected. This leads to a steep decrease in the upper bound. On the lower bound, when disruption severity is relatively low (n < 7), the bridges in group C, especially bridge C5, are identified as important links as their disruptions can lead to the worst case. This could be explained based on the network topology. The connectivity of O-D pairs between regions 2 and 3 largely depends on the bridges in Group C. There are no alternative bridges for C5 when θ = 2.0, as C5 is relatively far away from its adjacent bridges (C4 and C6) compared with other bridges. However, the worst-case disruption pattern is completely changed at n = 7. The bridges in groups A and B become more important as they together determine the connectivity of O-D pairs from/to region 1. When n = 9, all bridges in groups A and B are disrupted, which can disconnect all routes between region 1 and the other regions.

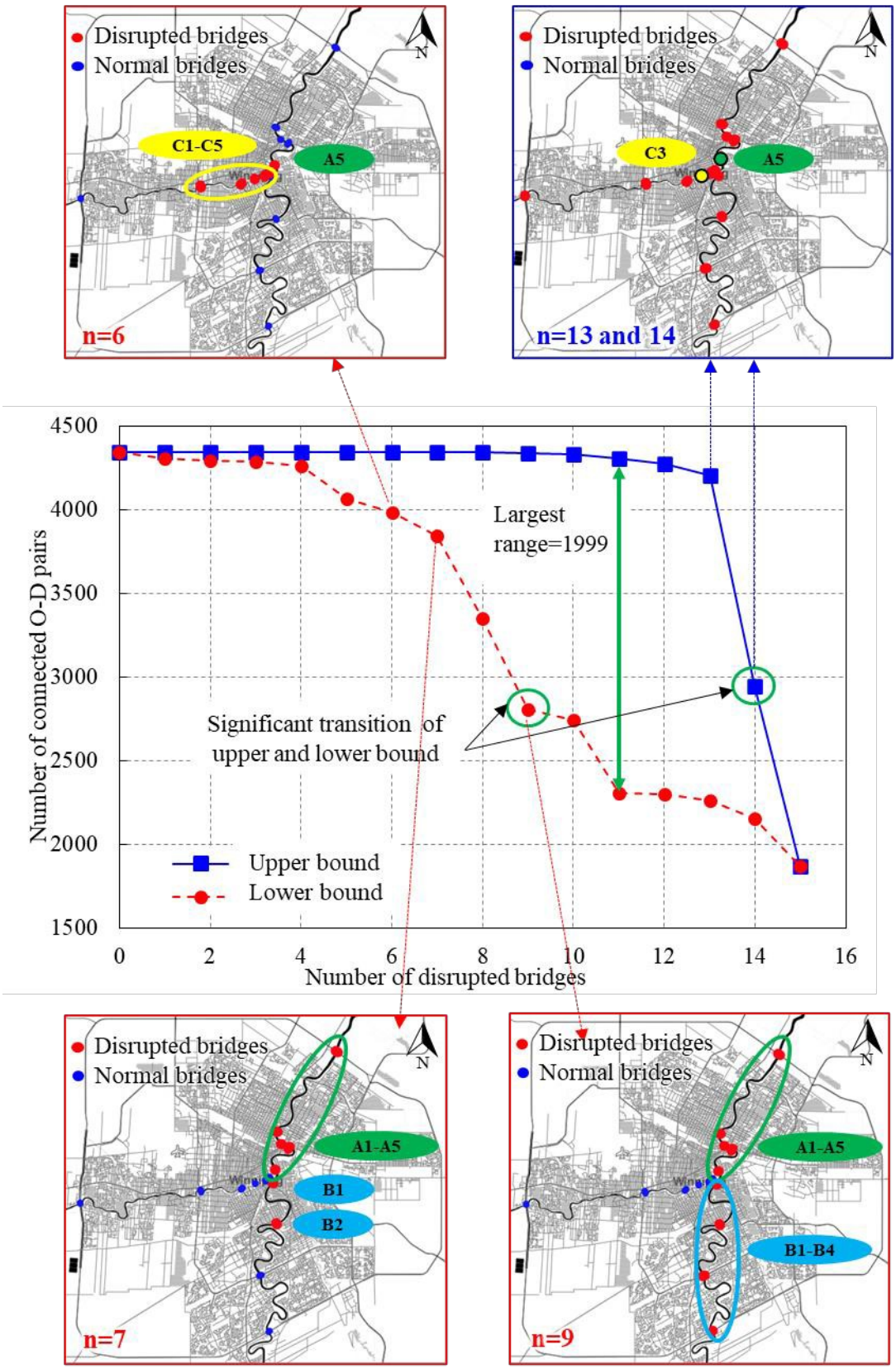

Figure 12. TNVE of the Winnipeg network under various bridge disruption scenarios

4.3.2 Vulnerability envelope buffer and sub-important bridges

The proposed method is also capable of generating a pool of solutions at each generation, from which we can obtain a variety of alternative good solutions, although not necessarily optimal, to the TNVE model. These solutions provide near-optimal lower and upper bounds and sub- important link combinations, which play a critical role in network vulnerability analysis (Gu et al., 2023). The features and effects of deriving multiple alternative solutions are illustrated in Figure 13. First, we show the envelope buffer (difference in network performances) between the optimal and near-optimal vulnerability bounds found by the proposed method. Larger buffers are found on the lower bounds, while the buffers on the upper bounds are mainly negligible. Furthermore, buffers become significant when the lower bound is steep, e.g., in the severity segment from $n = 5$ to $n = 9$. Then, we demonstrate the effects of multiple solutions by identifying the most and sub-important bridge combinations from the top 10 solutions at $n = 9$ (i.e., the solutions with the top 10 lowest objective values), where the largest buffer is found. Comparing to the optimal solution which disrupts all bridges in groups A and B, the near- optimal solutions either close bridges in Group C (solutions 2, 4, 5) instead of bridges in Group B, or replace one bridge in Group B (B4) by one bridge in Group C (solutions 3 and 6-10). These near-optimal solutions can provide distinct bridge combinations that are worth reinforcement or protection in practice. In addition, the difference between the objective values of different solutions implies the difference in the importance of bridge combinations. For instance, the difference between solutions 1 and 2 indicates that closing bridges in Group C instead of Group B may cause at least 319 fewer O-D disconnections. The comparison between solutions 1 and 3 shows that the extreme case given by the optimal solution only takes place when a whole group of bridges are simultaneously disrupted. If one bridge in another group is closed instead of B4 in Group B, at least 458 more O-D pairs remain connected. Therefore, in addition to focusing on the worst cases which can only be triggered by the extreme disruption scenarios that are less likely to happen, it is also worthwhile to consider the sub-optimal bridges with great impacts on more general but still severe near-extreme cases.

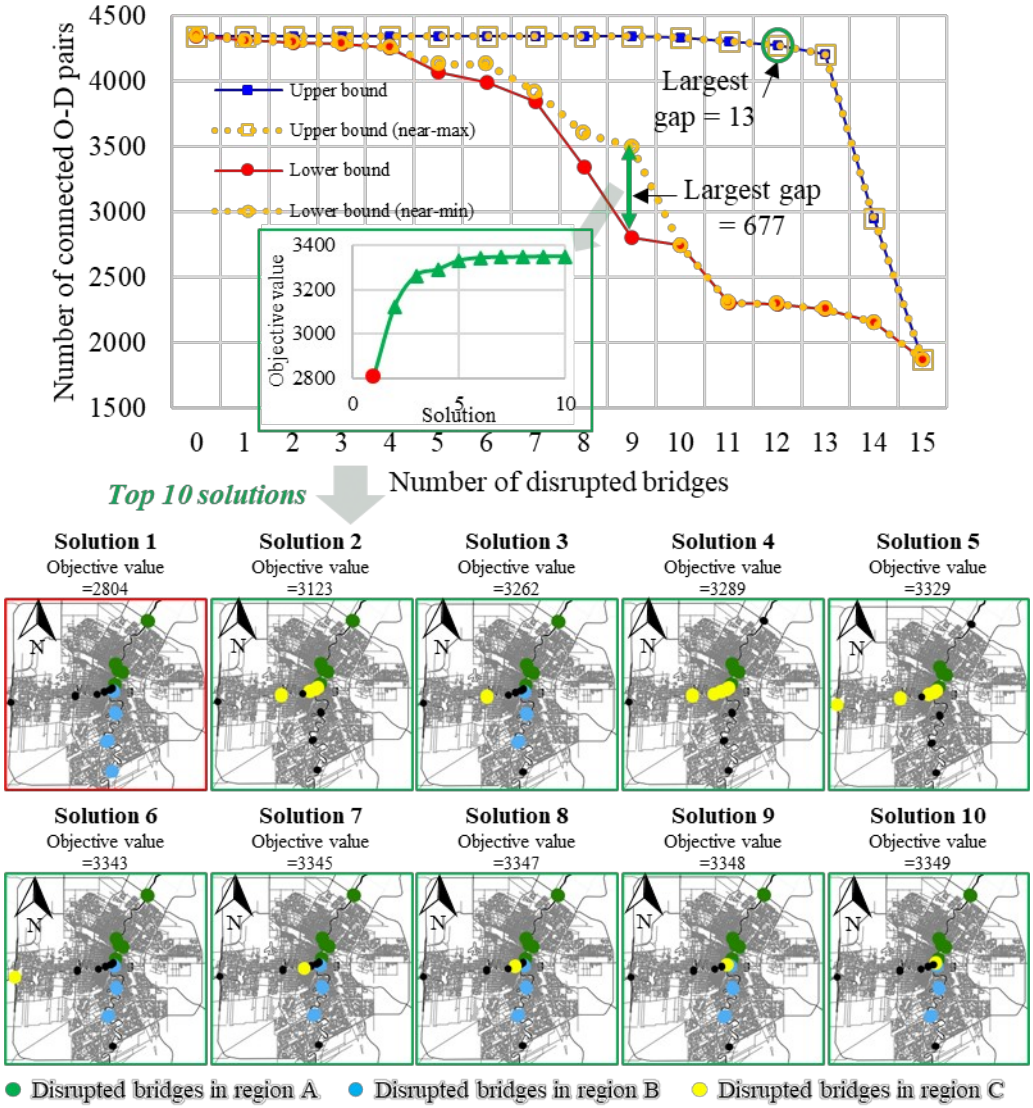

Figure 13. TNVE buffer and corresponding optimal and near-optimal solutions

4.3.3 Sensitivity analysis of acceptable elongation ratio

The acceptable elongation ratio θ is an important factor reflecting the required service level in the post-disruption transportation network. In this section, we conduct a sensitivity analysis for understanding the possible changes in vulnerability bounds and ranges with respect to different elongation ratios. Specifically, we examine the TNVEs under θ = 1.0, 2.0, and 10.0. If θ = 1.0, only the shortest path is acceptable between each O-D pair; while θ = 2.0 and θ = 10.0 respectively indicate that travelers can accept two and ten times as long as the shortest path between each O-D pair. As shown in Figures 14(a)-(c), both upper and lower bounds rise with the increase of θ (i.e., more O-D pairs are considered as connected when the elongation requirement is relaxed). An obvious difference between θ =1.0 and θ =2.0 is that the upper bound of θ = 2.0 becomes flat under simultaneous disruptions of 1 to 13 bridges (as opposed to a linear decreasing rate), while the lower bound of θ = 2.0 generally decreases at a linear rate (as opposed to a nonlinear decreasing rate) from 6 to 10 disrupted bridges. When θ is further relaxed to 10, the difference between the upper and lower bounds is negligible under disruptions of 1 to 8 bridges, as the two bounds are identically flat.

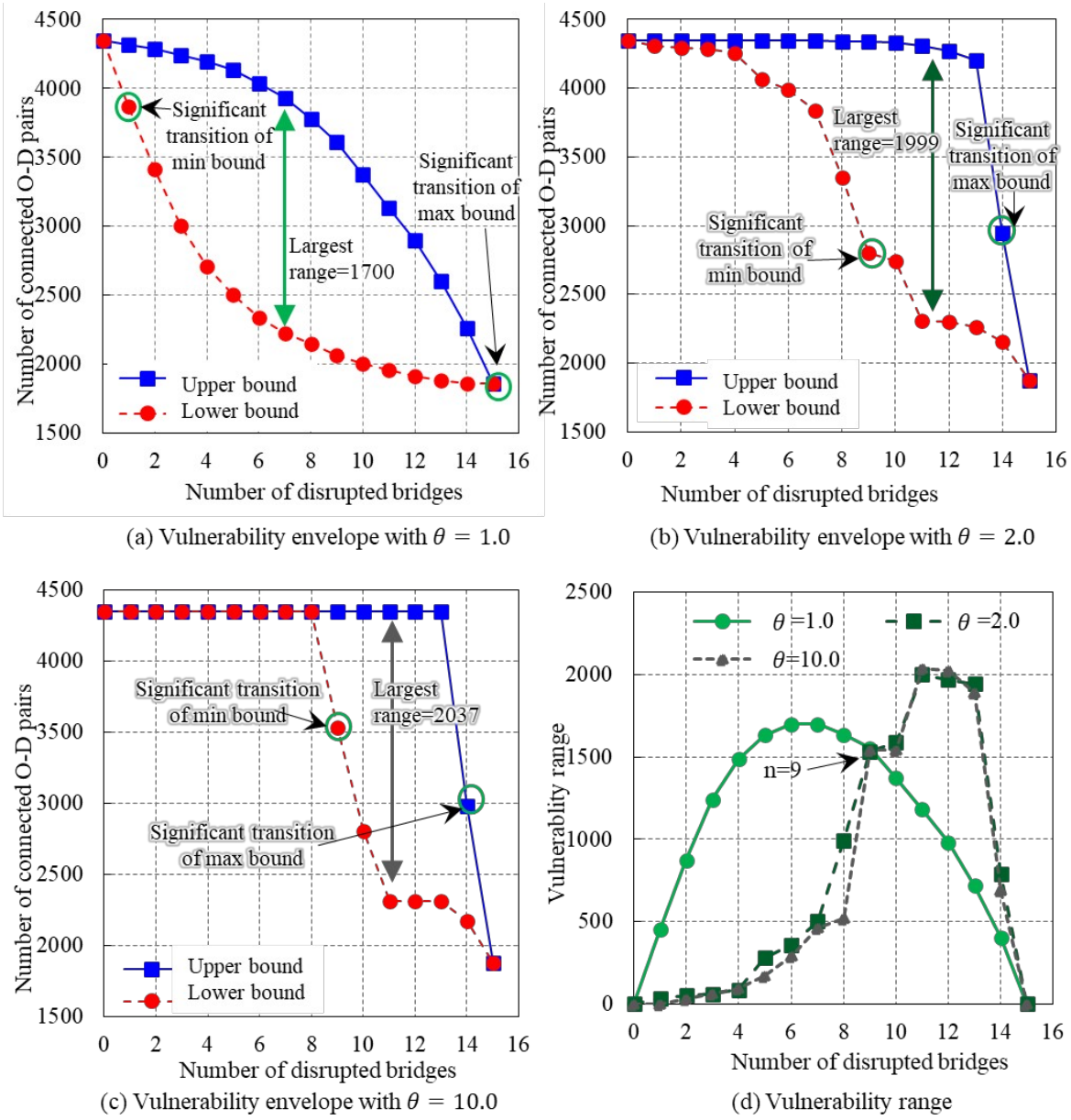

Figure 14. Vulnerability envelops with different elongation parameters

As can be seen from Figure 14(d), different values of θ lead to obviously distinct patterns of vulnerability range. Furthermore, the evolution of vulnerability range changes at n = 9, the point at which the largest slope of the lower bound and the largest envelope buffer can be found. Before n = 9, a smaller value of θ (θ = 1.0) leads to a larger vulnerability range than a larger values of θ (θ = 2.0 or θ = 10.0). After n = 9, the range induced by a small θ is quickly decreasing, while the ranges led by larger values of θ continue to increase until n = 11. Overall, a restrictive requirement on the network service level (i.e., a low value of θ) tends to make the network evaluation outcomes sensitive to mild disruptions. This parameter setting can be used for network evaluation and decision-making in recurrent and non-severe perturbation conditions like heavy congestion and partial road closure caused by infrastructure maintenance. When longer detours are allowed, the uncertainty in network vulnerability is lower and the network is more likely to perform well under low disruption severities (i.e., n < 9). The critical points with significant changes in the slope of vulnerability bound, size of vulnerability range, and buffer between extreme and near-extreme cases can be more obviously observed under

severe disruptions. Therefore, the outcomes from a large θ are applicable to facilitate the decision-making oriented at non-recurrent disruptions with serious consequences, such as natural disasters and terrorist attacks.

5. Conclusion

This study develops a method based on the RKGA for solving the TNVE problem, which reveals not only the upper and lower bounds but also their buffers of transportation network performance under simultaneous disruptions of multiple links. The proposed method has two major computational benefits: (a) it derives the upper and lower vulnerability bounds simultaneously without the need to iteratively solve the TNVE model under a given disruption severity, and (b) it improves computational efficiency and guarantees solution feasibility by implicitly handling the cardinality constraint with respect to the number of disrupted links. The improved computational efficiency ensures the applicability to large-scale real-world transportation networks. In addition, the proposed method can provide a pool of solutions to the TNVE problem that reveals the TNVE buffers and identifies a variety of sub-important link combinations, which play a critical role in vulnerability-oriented decision-making (Gu et al., 2023). The numerical examples using the small and medium-sized networks demonstrate the effectiveness and efficiency of the proposed method. The numerical results of the Winnipeg network case study verify its applicability in large-scale real-world transportation networks. We observe that: (1) the rankings of link importance can be significantly different under different disruption severities due to the combinatorial complexity of the TNVE problem, (2) slightly altering the most important link combination may lead to much milder degradations than the extreme case, which implies the need of also considering the more likely sub-important links and TNVE buffers in TNVE analyses, and (3) the valuation of acceptable elongation ratio can significantly influence the TNVE analysis results and should be selected based on the targeted disruption scenarios.

The proposed study is still subject to several limitations. First, the present vulnerability envelope model focuses on the simultaneous independent disruptions of multiple network components, while the spatial-temporal correlations among infrastructures and their sequential disruptions are not considered in the analysis. It will be also interesting to account for the sequential disruptions (Ermagun et al., 2023a, 2023b), cascading effect (Duan et al., 2023), and spatial dependency among transportation infrastructures (Li et al., 2014; Esfeh et al., 2022). Second, this study investigates the vulnerability envelope under general disruptions. However, as shown in the TNVE buffer analysis, the probability that the post-disruption network performance reaches the upper/lower vulnerability bounds might be low in real-world events. It will be valuable to analyze the vulnerability envelope regarding specific disruptive events that are important to the studied transportation system, which calls for further considering the occurrence probability and probabilistic consequence of the targeted disruptions based on historical data (Esfeh et al., 2020, 2022). Third, the proposed method is mainly applied to road networks. It is necessary for TNVE analyses to also account for the topology and service features of urban rail transit networks (e.g., Ermagun et al., 2023a), which serves as the backbone of many densely populated megacities like Hong Kong.

Based on this study, a few directions are worthy of further investigation: (1) To extend the current application to a multi-modal transport network with public transit modes and emerging mobility services. (2) To further consider more behavioral features of travelers' rerouting under disruption, such as the congestion effect, inertia effect, and dynamic learning and choice

adjustment. (3) To consider more serviceability-based network performance measures for the TNVE analysis, such as system travel cost, network capacity, and utility-based accessibility.

Acknowledgments

The work described in this paper was jointly supported by the Research Grants Council of the Hong Kong Special Administrative Region (PolyU 15222221), and the Department of Civil and Environmental Engineering at the Hong Kong Polytechnic University (WZ06). In addition, the project 72071174 supported by the National Natural Science Foundation of China at the Hong Kong Polytechnic University Shenzhen Research Institute, Shenzhen, Guangdong, China is gratefully acknowledged.

References

Altarabsheh, A., Altarabsheh, I., and Ventresca, M. 2023. A hybrid genetic algorithm to maintain road networks using reliability theory. *Structure and Infrastructure Engineering*, 19(6), 810-823.

Andrade, C.E., Toso, R.F., Goncalves, J.F., and Resende, M.G.C. 2021. The multi-parent biased random-key genetic algorithm with implicit path-relinking and its real-world applications. *European Journal of Operational Research*, 289(1), 17-30.

Andrade, C.E., Silva, T., and Pessoa, L.S. 2019. Minimizing flowtime in a flowshop scheduling problem with a biased random-key genetic algorithm. *Expert Systems with Applications*, 128, 67–80.

Bean, J.C. 1994. Genetic algorithms and random keys for sequencing and optimization. *ORSA Journal on Computing*, 6(2), 154-160.

Bell, M.G.H. 2000. A game theory approach to measuring the performance reliability of transport networks. *Transportation Research Part B*, 34(6), 533–545.

Bell, M.G.H., Kanturska, U., Schmöcker, J.-D., and Fonzone, A. 2008 Attacker–defender models and road network vulnerability. *Philosophical Transactions: Mathematical, Physical and Engineering Sciences*, 366(1872), 1893–1906.

Berdica, K. 2002. An introduction to road vulnerability: What has been done, is done and should be done. *Transport Policy*, 9, 117–127.

Biajoli, F.L., Chaves, A.A., and Lorena, L.A.N. 2019. A biased random-key genetic algorithm for the two-stage capacitated facility location problem. *Expert Systems with Applications*, 115, 418−426.

Chen, A., Kim, J., Lee, S., and Kim, Y. 2010a. Stochastic multi-objective models for network design problem. *Expert Systems with Applications*, 37, 1608–1619.

Chen, A., Subprasom, K., and Ji, Z. 2006. A simulation-based multi-objective genetic algorithm (SMOGA) procedure for BOT network design problem. *Optimization and Engineering*, 7, 225–247.

Chen, A., and Xu, X. 2012. Goal programming approach to solving network design problem with multiple objectives and demand uncertainty. *Expert Systems with Applications*, 39, 4160–4170.

Chen, A., Yang, C., Kongsomsaksakul, S., and Lee, M. 2007. Network-based acessibility measures for vulnerability analysis of degradable transportation networks. *Networks and Spatial Economics*, 7, 241–256.

Chootinan, P., Chen, A., Horrocks, M.R., Bolling, D., 2006. A multi-year pavement maintenance program using a stochastic simulation-based genetic algorithm approach. *Transportation Research Part A*, 40, 725–743.

Chootinan, P., Chen, A., Yang, H., 2005. A bi-objective traffic counting location problem for origin-destination trip table estimation. *Transportmetrica*, 1, 65–80.

Connors, R.D., and Watling, D.P. 2015. Assessing the demand vulnerability of equilibrium traffic networks via network aggregation. *Networks and Spatial Economics*, 15, 367-395.

De Freitas, C.C., Aloise, D.J., Da Costa Fontes, F.F., Santos, A.C., and Da Silva Menezes, M. 2023. A biased random‐key genetic algorithm for the two‐level hub location routing problem with directed tours. *OR Spectrum*, https://doi.org/10.1007/s00291-023-00718-y.

Du, M., Jiang, X., and Chen, A. 2022. Identifying critical links using network capacity-based indicator in multi-modal transportation networks. *Transportmetrica B*, 10(1), 1126-1150.

Duan, J., Li, D., and Huang, H-J. 2023. Reliability of the traffic network against cascading failures with individuals acting independently or collectively. *Transportation Research Part C*, 147, 104017.

Ermagun, A., Tajik, N., Janatabadi, F., and Mahmassani, H. 2023a. Uncertainty in vulnerability of metro transit networks: A global perspective. *Journal of Transport Geography*, 113, 103710.

Ermagun, A., Tajik, N., and Mahmassani, H. 2023b. Uncertainty in vulnerability of networks under attack. *Scientific Reports*, 13(1), 3179.

Esfeh, M.A., Kattan, L., Lam, W.H., Esfe, R.A., and Salari, M. 2020. Compound generalized extreme value distribution for modeling the effects of monthly and seasonal variation on the extreme travel delays for vulnerability analysis of road network. *Transportation Research Part C*, 120, 102808.

Esfeh, M.A., Kattan, L., Lam, W.H., Salari, M., and Esfe, R.A. 2022. Road network vulnerability analysis considering the probability and consequence of disruptive events: A spatiotemporal incident impact approach. *Transportation Research Part C*, 136, 103549.

Gen, M., and Cheng, R. 1999. Genetic Algorithms and Engineering Optimization, Wiley Series in Engineering Design and Automation. John Wiley & Sons, Inc., Hoboken, NJ, USA.

Goldberg, D.E., and Holland, J.H. 1988. Genetic Algorithms and Machine Learning. *Machine Learning*, 3, 95–99.

Gonçalves, J.F., and Resende, M.G.C. 2011. Biased random-key genetic algorithms for combinatorial optimization. *Journal of Heuristics*, 17, 487–525.

Gu, Y., Chen, A., and Li, G. 2022. Sensitivity analysis-based multi-modal transportation network vulnerability assessment with weibit choice models. The 13th International Conference on Reliability, Maintainability, and Safety (ICRMS), Hong Kong, August 21- 24.

Gu, Y., Chen, A., and Xu, X. 2023. Measurement and ranking of important link combinations in the analysis of transportation network vulnerability envelope buffers under multiple-link disruptions. *Transportation Research Part B*, 167, 118-144.

Gu, Y., Fu, X., Liu, Z., Xu, X., and Chen, A. 2020. Performance of transportation network

under perturbations: Reliability, vulnerability, and resilience. *Transportation Research Part E*, 133, 1–16.

Hien, V.Q., Dao, T.C., and Binh, H.T.T. 2023. A greedy search based evolutionary algorithm for electric vehicle routing problem. *Applied Intelligence*, 53, 2908–2922.

Huang, W., Li, L., Liu, H., Zhang, R., and Xu, M. 2021. Defense resource allocation in road dangerous goods transportation network: A self-contained Girvan-Newman algorithm and mean variance model combined approach. *Reliability Engineering & System Safety*, 215, 107899.

Jansuwan, S., and Chen, A. 2015. Considering perception errors in network efficiency measure: an application to bridge importance ranking in degradable transportation networks. *Transportmetrica A*, 11, 793–818.

Jenelius, E., Petersen, T., and Mattsson, L.G. 2006. Importance and exposure in road network vulnerability analysis. *Transportation Research Part A*, 40, 537-560.

Ji, Z., Kim, Y.S., and Chen, A. 2011. Multi-objective α-reliable path finding in stochastic networks with correlated link costs: A simulation-based multi-objective genetic algorithm approach (SMOGA). *Expert Systems with Applications*, 38, 1515–1528.

Karakatič, S. 2021. Optimizing nonlinear charging times of electric vehicle routing with genetic algorithm. *Expert Systems with Applications*, 164, 114039.

Li, D., Jiang, Y., Kang, R., and Havlin, S. 2014. Spatial correlation analysis of cascading failures: Congestions and blackouts. *Scientific Reports*, 4(1), 5381.

Li, Z., Jin, C., Hu, P., and Wang, C. 2019. Resilience-based transportation network recovery strategy during emergency recovery phase under uncertainty. *Reliability Engineering & System Safety*, 188, 503–514.

Liu, M., Wang, D., Zhao, J., and Si, S. 2022. Importance measure construction and solving algorithm oriented to the cost-constrained reliability optimization model. *Reliability Engineering & System Safety*, 222, 108406.

Londe, M.A., Andrade, C.E., and Pessoa, L.S. 2021 An evolutionary approach for the p-next center problem. *Expert Systems with Applications*, 175, 114728.

Luathep, P., Sumalee, A., Ho, H.W., and Kurauchi, F. 2011. Large-scale road network vulnerability analysis: a sensitivity analysis based approach. *Transportation*, 38(5), 799–817.

Mattsson, L.G., and Jenelius, E. 2015. Vulnerability and resilience of transport systems - A discussion of recent research. *Transportation Research Part A*, 81, 16–34.

Mendes, J.J.M., Gonçalves, J.F., and Resende, M.G.C. 2009. A random key based genetic algorithm for the resource constrained project scheduling problem. *Computers & Operations Research*, 36, 92–109.

Nicholson, A., and Du, Z.P. 1997. Degradable transportation systems: an integrated equilibrium model. *Transportation Research Part B*, 31(3), 209–223.

Nunes, P., Moura, A., and Santos, J. 2023. Solving the multi-objective bike routing problem by meta-heuristic algorithms. *International Transactions in Operational Research*, 30, 717–741.

Paulavičius, R., Stripinis, L., Sutavičiute, S., and Kočegarov, D. 2023. A novel greedy genetic algorithm-based personalized travel recommendation system. *Expert Systems with Applications*, 230, 120580.

Platt, R.H. 1991. Lifelines: An emergency management priority for the United States in the 1990s. *Disasters*, 15, 172–176.

Qiang, Q., and Nagurney, A. 2008. A unified network performance measure with importance identification and the ranking of network components. *Optimization Letters*, 2(1), 127-142.

Rajabi-Bahaabadi, M., Shariat-Mohaymany, A., Babaei, M., and Ahn C.W. 2015. Multi-objective path finding in stochastic time-dependent road networks using non-dominated sorting genetic algorithm. *Expert Systems with Applications*, 42, 5056–5064.

Ruiz, E., Soto-Mendoza, V., Barbosa, A.E.R., and Reyes, R. 2019. Solving the open vehicle routing problem with capacity and distance constraints with a biased random key genetic algorithm. *Computers & Industrial Engineering*, 133, 207-219.

Ryu, S., Chen, A., Xu, X., and Choi, K. (2018). Solving transport network vulnerability envelope under simultaneous multi-link disruptions: A random key genetic algorithm. Presented at *the 7th International Symposium on Transport Network Reliability*.

Samanlioglu, F., Ferrell, W.G., and Kurz, M.E. 2008. A memetic random-key genetic algorithm for a symmetric multi-objective traveling salesman problem. *Computers & Industrial Engineering*, 55, 439–449.

Salman, S., and Alaswad, S. 2022. Designing reduced congestion road networks via an elitist adaptive chemical reaction optimization. *Computers & Industrial Engineering*, 163, 107788.

Snyder, L.V., and Daskin, M.S. 2006. A random-key genetic algorithm for the generalized traveling salesman problem. *European Journal of Operational Research*, 174, 38–53.

Sun, W., Shao, H., Shen, L., Wu, T., Lam, W.H.K., Yao, B., and Yu, B. 2021. Bi-objective traffic count location model for mean and covariance of origin–destination estimation. *Expert Systems with Applications*, 170, 114554.

Szeto, W.Y. 2011. Cooperative game approaches to measuring network reliability considering paradoxes. *Transportation Research Part C*, 19(2), 229-241.

Taylor, M.A.P. 2017. Vulnerability Analysis for Transportation Networks. Oxford: Elsevier.

Wang, D.Z.W., Liu, H., Szeto, W.Y., and Chow, A.H.F. 2016. Identification of critical combination of vulnerable links in transportation networks – A global optimisation approach. *Transportmetrica A*, 12, 346–365.

Xie, Y., Sheng, Y., Qiu, M., and Gui, F. 2022. An adaptive decoding biased random key genetic algorithm for cloud workflow scheduling. *Engineering Applications of Artificial Intelligence*, 112, 104879.

Xu, X., Chen, A., and Yang, C. 2018. An optimization approach for deriving upper and lower bounds of transportation network vulnerability under simultaneous disruptions of multiple links. *Transportation Research Part C*, 94, 338–353.

Xu, X., Chen, A., Xu, G., Yang, C., and Lam, W.H.K. 2021. Enhancing network resilience by

adding redundancy to road networks. *Transportation Research Part E,* 154, 102448.

Yang, C., and Chen, A. 2009. Sensitivity analysis of the combined travel demand model with applications. *European Journal of Operational Research*, 198(3), 909-921,

Zhou, S., Xie, J., Du, N, and Pang, Y. 2018. A random-keys genetic algorithm for scheduling unrelated parallel batch processing machines with different capacities and arbitrary job sizes. *Applied Mathematics and Computation*, 334, 254-268.

Zhou, S., Ji, B., Song, Y., Yu, S.S., Zhang, D., Van Woensel, T. 2023. Hub-and-spoke network design for container shipping in inland waterways. *Expert Systems with Applications*, 223, 119850.

Ziar, E., Seifbarghy, M., Bashiri, M., and Tjahjono, B. 2023. An efficient environmentally friendly transportation network design via dry ports: A bi-level programming approach. *Annals of Operations Research*, 322, 1143–1166.